

MOL#108605

## Title Page

# **A novel selective inverse agonist of the CB2 receptor as a radiolabeled tool compound for kinetic binding studies.**

Andrea Martella, Huub Sijben, Arne C. Rufer, Uwe Grether, Juergen Fingerle, Christoph Ullmer, Thomas Hartung, Adriaan P. IJzerman, Mario van der Stelt and Laura H. Heitman

Division of Medicinal Chemistry, Leiden Academic Centre for Drug Research, Leiden University, Leiden, The Netherlands (A.M., H.B., A.P.I., L.H.H.); Roche Pharma Research and Early Development, pRED, Roche Innovation Center Basel, F. Hoffmann-La Roche Ltd., Basel, Switzerland (A.M., A.C.R., U.G., C.U., T.H.); Department of Molecular Physiology, Leiden Institute of Chemistry, Leiden University, Leiden, The Netherlands (A.M., M.S.); NMI, Natural and Medical Sciences Institute, University of Tübingen, Reutlingen, Germany (J.F.).

MOL#108605

## Running title page

**Running Title:** A novel tool compound for CB<sub>2</sub> kinetic binding studies

**Corresponding author:** Laura H. Heitman, Ph.D., Associate Professor for Molecular Pharmacology

Email: l.h.heitman@lacdr.leidenuniv.nl; Address: Einsteinweg 55, 2333 CC Leiden, The Netherlands;  
Telephone: +31(0)71 527 4558

**Pages number:** 26

**Figures number:** 8

**Tables number:** 2

**References:** 66

**Abstract words count:** 248

**Introduction words count:** 754

**Discussion words count:** 1438

### Abbreviations:

ECS: Endocannabinoid system

CB1R: Cannabinoid 1 receptor

CB2R: Cannabinoid 2 receptor

GPCR: G protein-coupled receptor

AEA: *N*-arachidonylethanolamine

2-AG: 2-arachidonoylglycerol

CNS: Central nervous system

RT: residence time

PET: positron emission tomography

PEI: polyethylenimine

NE: Noladin ether

CHO: Chinese hamster ovary

TB: total binding

NSB: non-specific binding

FB: filter binding

MOL#108605

## Abstract

The endocannabinoid system (ECS) and in particular the cannabinoid receptor 2 (CB2R), raised the interest of many medicinal chemistry programs for its therapeutic relevance in several (patho)physiological processes. However, the physico-chemical properties of tool compounds for CB2R (e.g. the radioligand [ $^3\text{H}$ ]CP55,940) are not optimal, despite the research efforts in developing effective drugs to target this system. At the same time, the importance of drug-target binding kinetics is growing, as the kinetic binding profile of a ligand may provide important insights for the resulting *in vivo* efficacy. In this context we synthesized and characterized [ $^3\text{H}$ ]RO6957022, a highly selective CB2R inverse agonist, as a radiolabeled tool compound. In equilibrium and kinetic binding experiments [ $^3\text{H}$ ]RO6957022 showed high affinity for human CB2R with fast association ( $k_{\text{on}}$ ) and moderate dissociation ( $k_{\text{off}}$ ) kinetics. To demonstrate the robustness of [ $^3\text{H}$ ]RO6957022 binding, affinity studies were carried out for a wide range of CB2R reference ligands, spanning from full, partial to inverse agonists. Finally, we used [ $^3\text{H}$ ]RO6957022 to study the kinetic binding profiles (i.e.  $k_{\text{on}}$  and  $k_{\text{off}}$  values) of selected synthetic and endogenous (i.e. 2-arachidonoylglycerol, anandamide and noladin ether) CB2R ligands by competition association experiments. All tested ligands, and in particular the endocannabinoids displayed distinct kinetic profiles, shedding more light on their mechanism of action and the importance of association rates in the determination of CB2R affinity. Altogether, this study shows that the use of a novel tool compound, i.e. [ $^3\text{H}$ ]RO6957022, can support the development of novel ligands with a repertoire of kinetic binding profiles for CB2R.

MOL#108605

## Introduction

Historically, the plant *Cannabis sativa* and its preparations have been exploited for millennia, finding its use in medical and recreational applications (Mechoulam et al., 2014). Since the structural characterization of  $\Delta^9$ -tetrahydrocannabinol ( $\Delta^9$ -THC), the main psychoactive constituent of cannabis, in 1964 (Gaoni and Mechoulam, 1964), two class A G protein-coupled receptors (GPCRs) have been identified as a target of  $\Delta^9$ -THC, namely cannabinoid receptor type 1 (CB1R) (Devane et al., 1988) and type 2 (CB2R) (Munro et al., 1993). The presence of these GPCRs implied the existence of endogenous ligands, which were identified as signaling lipids derived from arachidonic acid [i.e. *N*-arachidonylethanolamine (AEA) and 2-arachidonoylglycerol (2-AG)]. These bioactive lipids were coined as endocannabinoids (Di Marzo and Fontana, 1995). More recently, a complete enzymatic machinery was found to control the levels of these endocannabinoids that are synthesized and degraded in an “on demand” fashion after various types of stimuli (Ligresti et al., 2016).

The two CBRs are expressed in different cellular systems throughout the human body and are involved in various physiological and pathological processes. CB1R is mainly expressed in the central nervous system (CNS) and to a lesser extent in peripheral tissue, whereas the CB2R is thought to be primarily expressed in immune cells (e.g. B and T lymphocytes, monocytes, macrophages) (Galiegue et al., 1995; Turcotte et al., 2016).

Since its discovery, CB2R has become an interesting anti-inflammatory target in a variety of disease areas (Dhopeswarkar and Mackie, 2014; Picone and Kendall, 2015), including pain (Anand et al., 2009; Guindon and Hohmann, 2008), neurological disorders (e.g. Parkinson's, Huntington's) (Aso et al., 2013; Cabral et al., 2008; Fernandez-Ruiz et al., 2011), osteoporosis (Ofek et al., 2006), nephropathy (Mukhopadhyay et al., 2016; Mukhopadhyay et al., 2010), hepatic diseases (Lotersztajn et al., 2008), and ischemia reperfusion injury (Horvath et al., 2012; Li et al., 2013). Hence, considerable effort has been put into the synthesis and preclinical screening of novel CB2R selective ligands, where the *in vivo* application of some of these has already generated some promising results (Morales et al., 2016; Riether, 2012). However, in spite of these efforts, no CB2R ligands have shown

MOL#108605

efficacy in clinical trials so far (Dhopeshwarkar and Mackie, 2014). Poor *in vitro* characterization of the drug candidates, ambiguous findings in animal models (Moris et al., 2015) and low interspecies CB2R homology (Brown et al., 2002), could have contributed to these failures in clinical trials, and novel approaches are needed to bridge this translational gap (Soethoudt et al., 2017).

A decade ago, the concept of drug-target binding kinetics was introduced as a means to better predict the *in vivo* efficacy of ligands, in addition to conventional lead optimization parameters like ligand affinity and potency (Copeland et al., 2006). The concept takes into account the receptor recognition of the ligand, defined by the association rate ( $k_{on}$ , in  $\text{nM}^{-1} \text{min}^{-1}$ ) and the ligand-receptor complex stability, defined by the dissociation rate ( $k_{off}$ , in  $\text{min}^{-1}$ ). These kinetic parameters hold important information that can be related to a drug's *in vivo* efficacy. For instance, the residence time (RT) which is defined as the reciprocal of  $k_{off}$ , is a measure of the stability of the ligand-receptor complex and has been shown (retrospectively) to correlate with drug efficacy and safety (Tummino and Copeland, 2008). In addition, recent studies outlined the importance of a high  $k_{on}$  value as an important determinant to achieve sufficient target occupancy (de Witte et al., 2016) by means of rebinding and micro-pharmacokinetic processes (Sykes et al., 2014; Vauquelin, 2016).

To the best of our knowledge, there have been no reports on CB2R ligand binding kinetics yet. Therefore, applying this novel approach to study the CB2R kinetic binding behavior of endogenous and synthetic ligands could be give important insights for cannabinoid receptor drug research.

With respect to the classic filtration binding assay typically performed with the unselective [ $^3\text{H}$ ]CP55,940, kinetic binding experiments require a more robust radiolabeled tool compound with low non-specific binding. In this study, we describe the characterization of [ $^3\text{H}$ ]RO6957022 (Figure 1), a novel tritiated compound with nanomolar affinity, inverse agonist behavior and high selectivity for CB2R (Slavik et al., 2015). This compound is based on a 2,5,6-substituted pyridine scaffold and was previously reported as a positron emission tomography (PET) imaging probe in a [ $^{11}\text{C}$ ]-labeled form (Slavik et al., 2015). To support its relevance as an *in vitro* binding kinetics tool compound, we used it to determine the kinetic binding profile of chemically diverse CB2R ligands ranging from full,

MOL#108605

partial to inverse agonists. Moreover, this paper describes for the first time the binding kinetics of endocannabinoids on CB2R.

## Materials and Methods

*Chemicals and reagents-* Bovine serum albumin (BSA), polyethylenimine (PEI), CP55,940, GW405833, AM1241 and AM630 were purchased from Sigma Aldrich (St. Louis, MO, USA). JWH-133, HU-308, anandamide, 2-AG and noladin ether (NE) were supplied by Tocris Bioscience (Bristol, UK). Bicinchoninic acid (BCA) protein assay reagent were purchased from Pierce Chemical Co. (Rockford, IL, USA). SR144528 was purchased from Santa Cruz Biotechnology (Dallas, TX, USA). LEI-101 was provided by Baggelaar M. from Molecular physiology group (Leiden Institute of Chemistry, Leiden University). PathHunter®  $\beta$ -Arrestin CHO-K1 cells stably expressing human CB2R (CHO-K1\_hCB<sub>2</sub>) were purchased from DiscoverX (Fremont, CA, USA). All other chemicals were of analytical grade and obtained from commercial sources.

*Cell culture and membrane preparation-* CHO-K1\_hCB<sub>2</sub> were cultured in Dulbecco's Modified Eagle's media/ nutrient F-12 Ham 1:1 mixture (Sigma) supplemented with 10% fetal calf serum (Sigma), 300  $\mu$ g/mL hygromycin (InvivoGen), 800  $\mu$ g/mL G418 (Duchefa Biochemie), 100  $\mu$ g/mL penicillin/streptomycin (Duchefa Biochemie) and Glutamax (Gibco) at 37 °C and 5% CO<sub>2</sub>. Cells were subcultured twice a week at 90% confluency. Confluent cells were trypsinized and pooled. Subsequently, cells were pelleted and resuspended in ice-cold buffer (50 mM Tris-HCl at pH 7.4) and homogenized using an Ultra Turrax (IKA-Werke GmbH & Co. KG, Staufen, Germany). CHO-K1\_hCB<sub>2</sub> membranes were obtained by a double centrifugation step at 100,000 g at 4°C for 20 minutes (Optima LE-80K ultracentrifuge [Beckman Coulter]), after which the suspension was aliquoted and stored at -80°C until further use. Just prior to use membranes were thawed, homogenized using an Ultra Turrax and diluted to 60  $\mu$ g/ml with ice cold assay buffer (Tris-HCl 50 mM, pH 7.4 and 0.1% BSA). Protein concentrations were determined for each batch of membranes by a BCA protein assay (Smith et al., 1985).

MOL#108605

*Preparation of [<sup>3</sup>H]RO6957022*- A solution of 870 µg (2.14 µmol) of the O-desmethyl precursor 3-ethyl-2-(6-(cyclopropylmethoxy)-5-(3-hydroxyazetidin-1-yl)picolinamido)-2-ethylbutanoate and 1.43 µmol of LiHMDS (1 M in THF) in 100 µl of DMF is added to 50 mCi (1.85 GBq, 0.714 µmol) of [<sup>3</sup>H]-methyl nosylate in a 1 ml reaction vial. After stirring for 16 hours at room temperature the reaction mixture is treated with 5 ml of water and extracted 3-times with 4 ml of TBME. The organic layers are separated, dried over sodium sulfate, and the solvent is removed in vacuum. The crude product is purified by flash chromatography (silica, AcOEt / n-heptane 1:4) to yield 4.2 mCi (8.4%) of the tritium labeled radioligand in 96.7% radiochemical purity and a specific activity of 83.7 Ci/mmol (3.1 TBq/mmol). Radiochemically highly pure material (> 99%) can be obtained by additional HPLC purification (Waters XBridge C18, acetonitrile/water 30/70 to 90/10 over 20 min).

*Saturation binding experiments with [<sup>3</sup>H]RO6957022*- In saturation experiments, CHO-K1\_hCB<sub>2</sub> membranes (1.5 µg per well) were incubated with radioligand in assay buffer (Tris-HCl 50 mM, pH 7.4 and 0.1% BSA) at 25°C for 90 minutes (to ensure equilibrium was reached at all radioligand concentrations). Total binding (TB) was determined by increasing concentrations of [<sup>3</sup>H]RO6957022 between 0.3 and 18 nM, whereas non-specific binding (NSB) was determined at three concentrations of radioligand in presence of AM630 (10 µM). Incubations were terminated by rapid filtration through a 96-well GF/C filter plate using a FilterMate 96-well plate harvester (Perkin-Elmer). The GF/C filters were pretreated with 0.25% PEI, 30 minutes prior to harvesting. Subsequently, filters were washed at least three times with ice cold assay buffer and then completely dried. Remaining radioactivity on the filter was detected by adding 25 µl Microscint™ scintillation cocktail to each well and counted using a MicroBeta<sup>2</sup>® 2450 Microplate Counter (Perkin-Elmer). Specific binding was obtained by linear subtraction of non-specific binding (NSB) from total binding (TB). For all the experiments TB was always <10% of the total amount of radioligand added to prevent ligand depletion. Moreover, [<sup>3</sup>H]RO6957022 did not significantly bind to control CHO-K1 membranes.

MOL#108605

*Displacement experiments with [<sup>3</sup>H]RO6957022*- In homologous and heterologous displacement experiments, CHO-K1\_hCB<sub>2</sub> membranes (1.5 µg per well) were incubated in assay buffer at 25°C with a fixed amount of [<sup>3</sup>H]RO6957022 (3 nM) in presence of increasing concentrations of unlabeled competing ligand. The dilution series of unlabeled competing ligand were dispensed by HP D300 digital dispenser (Tecan, Giessen, The Netherlands) and incubated until equilibrium was reached. Total binding was determined in the presence of buffer and set at 100%, while non-specific binding was determined in the presence of AM630 (10 µM) and set at 0%. Harvesting and counting procedures were performed as described in the “*Saturation binding experiments with [<sup>3</sup>H]RO6957022*” section.

*Association and dissociation experiments with [<sup>3</sup>H]RO6957022*- In association experiments, CHO-K1\_hCB<sub>2</sub> membranes (1.5 µg per well) were incubated in assay buffer at 25°C with a fixed amount of [<sup>3</sup>H]RO6957022 (3 nM) at different time points between 0 and 90 minutes. For dissociation experiments, membranes were incubated for 90 min in assay buffer at 25°C with a fixed amount of [<sup>3</sup>H]RO6957022 (3 nM). Subsequently, dissociation of [<sup>3</sup>H]RO6957022 was initiated by addition of 5 µL of an excess of AM630 (final concentration of 10 µM) to each well at different time points between 0 and 90 minutes. AM630 was chosen as a displacer of its inverse agonist nature and different chemical scaffold respect to RO6957022. Harvesting and counting procedures were performed as described in the “*Saturation binding experiments with [<sup>3</sup>H]RO6957022*” section.

*Competition association experiments with [<sup>3</sup>H]RO6957022*- The kinetic parameters of unlabeled competitor ligands were determined using the competition association assay as described by Motulsky and Mahan (Motulsky and Mahan, 1984). CHO-K1\_hCB<sub>2</sub> membranes (1.5 µg per well) were incubated in assay buffer at 25°C with a fixed amount of [<sup>3</sup>H]RO6957022 (3 nM) at different time points between 0 and 90 minutes in either absence (control) or presence of an unlabeled competing ligand. Assay validation was performed by homologous competition association, as described in the results section (Fig. 3). IC<sub>50</sub> concentrations of the unlabeled competitor ligands were used to obtain approximately 50% displacement of the radioligand after 90 minutes incubation with [<sup>3</sup>H]RO6957022. Appropriate vehicle controls (i.e. DMSO, ethanol and Tocrisolve™) were used according to the solvent used for each ligand. To prevent degradation of the endocannabinoids during the assay, 1 µM



MOL#108605

of phenylmethylsulfonyl fluoride was added to membrane preparations 30 minutes in advance of the assay. Harvesting and counting procedures were performed as described in the “*Saturation binding experiments with [<sup>3</sup>H]RO6957022*” section.

*Data analysis*- All data were analyzed using GraphPad Prism v7.00 for Windows (GraphPad Software, Inc., San Diego, CA, USA). The following equations were used to analyze the data and fit the curves. Application of the *F* test (Ludden et al., 1994) as implemented for comparison of nested models showed that a monophasic association model described the data sufficiently. When we considered two nested models, in which model 1 correspond to the simpler, we applied the following equation:  $F = [(SS_1 - SS_2)/(DF_1 - DF_2)] / (SS_2/DF_2)$  where SS is the sum of the squares and DF is the degrees of freedom for each model. For specific saturation binding of [<sup>3</sup>H]RO6957022 data was analyzed with the non-linear regression “one site- specific binding model” of GraphPad Prism, shown in the following equation:  $Y = B_{\max} * X / (K_D + X)$  where Y is the specific radioligand binding in pmol/mg protein,  $B_{\max}$  is the total amount of receptors, X depicts the [<sup>3</sup>H]RO6957022 concentration in nM and  $K_D$  the equilibrium affinity constant in nM. For homologous and heterologous displacement experiments data were analyzed with the “non-linear regression one site – fit logIC<sub>50</sub> model” shown in the following equation:  $Y = \text{Bottom} + (\text{Top} - \text{Bottom}) / (1 + 10^{(X - \log IC_{50})})$  where Y is the specific [<sup>3</sup>H]RO6957022 binding, Top and Bottom are plateau values of the curves both in the unit of Y, X represents the unlabeled competitor concentration in log M and logIC<sub>50</sub> the equilibrium affinity of the competing ligand used. Subsequently,  $K_i$  values were calculated using the Cheng-Prusoff equation (Cheng and Prusoff, 1973):  $K_i = IC_{50} / (1 + ([L] / K_D))$ , where [L] is the [<sup>3</sup>H]RO6957022 concentration in nM and  $K_D$  is the equilibrium affinity value of [<sup>3</sup>H]RO6957022 in nM. Association rate constants ( $k_{on}$ ) were determined by the following equation:  $k_{on} = (k_{obs} - k_{off}) / [L]$ , where [L] is the [<sup>3</sup>H]RO6957022 concentration in nM. Observed association rates ( $k_{obs}$ ) were determined with a one-phase exponential association analysis:  $Y = Y_0 + (\text{Plateau} - Y_0) * (1 - \exp(-k_{obs} * t))$ , where  $Y_0$  is the specific radioligand binding at time 0, Plateau represent the maximum specific [<sup>3</sup>H]RO6957022 binding at equilibrium,  $k_{obs}$  is the observed association rate in min<sup>-1</sup> and t is time in minutes. Dissociation rate constants ( $k_{off}$ ) were determined with a one-phase exponential decay analysis:  $Y =$

MOL#108605

$(Y_0 - \text{NSB}) * \exp(-k_{\text{off}} * t) + \text{NSB}$ , where  $k_{\text{off}}$  is the dissociation rate constant in  $\text{min}^{-1}$ . Data from homologous and heterologous competition association experiments were analyzed by the following equation (Motulsky and Mahan, 1984):  $[\text{RL}] = (\text{B}_{\text{max}}k_1[\text{L}] / K_F - K_S) * [(k_4(K_F - K_S) / (K_F K_S)) + ((k_4 - K_F) / K_F) * \exp(-K_F t) - ((k_4 - K_S) / K_S) * \exp(-K_S t)]$ , using the following variables:

$$K_A = k_1[\text{L}] + k_2$$

$$K_B = k_3[\text{I}] + k_4$$

$$K_F = 0.5 * [K_A + K_B + \sqrt{((K_A - K_B)^2 + 4 * k_1 k_3 [\text{L}][\text{I}])}]$$

$$K_S = 0.5 * [K_A + K_B - \sqrt{((K_A - K_B)^2 + 4 * k_1 k_3 [\text{L}][\text{I}])}]$$

Where  $[\text{RL}]$  is the amount of receptor-ligand complex,  $[\text{L}]$  is the concentration  $[\text{}^3\text{H}]\text{RO6957022}$  in nM,  $[\text{I}]$  depicts the concentration of unlabeled competitor in nM,  $K_A$  and  $K_B$  are the observed association ( $k_{\text{obs}}$ ) of  $[\text{}^3\text{H}]\text{RO6957022}$  and the unlabeled competitor,  $k_1$  and  $k_3$  the association rate constants ( $k_{\text{on}}$ ) of  $[\text{}^3\text{H}]\text{RO6957022}$  and the unlabeled competitor,  $k_2$  and  $k_4$  the dissociation rate constants ( $k_{\text{off}}$ ) of  $[\text{}^3\text{H}]\text{RO6957022}$  and the unlabeled competitor,  $t$  is the time in minutes. Receptor residence time was calculated by taking the reciprocal of the dissociation rate ( $1/k_{\text{off}}$ ) (Copeland et al., 2006). The correlation between two independent variables with Gaussian distribution was calculated by using the Pearson correlation coefficient ( $r$ ), with a two-tailed  $P$  value determination (Benesty et al., 2009).

## Results

*Assay binding optimization of  $[\text{}^3\text{H}]\text{RO6957022}$  to human CB2 receptor-* Initial experiments were focused on specific  $[\text{}^3\text{H}]\text{RO6957022}$  binding to human CB2R and to optimize the assay conditions for *in vitro* binding studies. Therefore, the presence of several additives were initially tested in a standard assay buffer (50 mM Tris HCl, pH 7.4) together with 3 nM of  $[\text{}^3\text{H}]\text{RO6957022}$  and CHO-K1\_hCB2 membranes (Fig. 2A). To reduce the NSB of  $[\text{}^3\text{H}]\text{RO6957022}$  to the GF/C filters during the harvesting

MOL#108605

process, the filters were pre-incubated for 30 minutes with PEI, which resulted in a dramatic decrease of the NSB, which was largely caused by filter binding (FB) of [<sup>3</sup>H]RO6957022 (Fig 1A). We thus concluded that the presence of 0.1% CHAPS or 0.1% w/v BSA (which we finally selected) in the assay buffer and pretreatment of the filters with 0.25% w/v of PEI was sufficient to provide a signal to noise ratio of [<sup>3</sup>H]RO6957022 binding of sufficient quality. Moreover, receptor specificity was confirmed by comparing the specific binding in CHO-K1\_hCB2 versus control CHO cells without overexpressing CB2R (Fig. 2B). Subsequently, membrane titration was performed to assess which concentration yielded an optimal window, i.e. big enough, but below the ligand depletion limit (i.e. 10% of total amount of radioligand present). Using 1.5 µg/ well of CHO-K1\_hCB<sub>2</sub> membranes we obtained approximately 4000 dpm of specific binding. As expected [<sup>3</sup>H]RO6957022 specific binding was directly correlated with the concentration of CHO-K1\_hCB2 membranes used (Fig. 2B), while NSB was not affected, indicating that this residual binding was indeed mostly caused by the filter.

*[<sup>3</sup>H]RO6957022 saturation experiment to human CB<sub>2</sub> receptor-* To confirm the affinity of [<sup>3</sup>H]RO6957022 for CB2R, we performed equilibrium saturation binding experiments (Fig. 3A). Binding of [<sup>3</sup>H]RO6957022 to CHO-K1 hCB<sub>2</sub> membranes was saturable and best described by a one-site model. The equilibrium dissociation constant (K<sub>D</sub>) of [<sup>3</sup>H]RO6957022 was found to be 1.7 ± 0.1 nM, with a receptor density (B<sub>max</sub>) value of 25 ± 1 pmol/mg protein in the membranes used (Table 1).

*Equilibrium displacement assay using [<sup>3</sup>H]RO6957022 and CB2R reference ligands-* Next, [<sup>3</sup>H]RO6957022 was used to perform displacement experiments with eight previously reported orthosteric CB2R ligands (Fig. 1). These included agonists (CP55,940, JWH-133, AM1241, HU-308), a partial agonist (GW405833) and inverse agonists (SR144528, AM630). All compounds tested were able to fully displace [<sup>3</sup>H]RO6957022 from the orthosteric binding site with nanomolar affinities (Table 2 and Fig. 4). In addition, we performed a homologous displacement assay with RO6957022, which resulted in an affinity of 1.3 nM (pK<sub>i</sub>= 8.9) for the unlabeled compound, i.e. similar to its equilibrium K<sub>D</sub> value determined from [<sup>3</sup>H]RO6957022 saturation experiments (Fig. 1, Table 1).

MOL#108605

*Kinetic characterization of [<sup>3</sup>H]RO6957022 on human CB<sub>2</sub> receptor-* Subsequently, the association ( $k_{on}$ ) and dissociation ( $k_{off}$ ) rate constants of [<sup>3</sup>H]RO6957022 were determined (Table 2 and Fig. 3B). The binding of [<sup>3</sup>H]RO6957022 reached equilibrium after approximately 10 min at 25°C. Specific [<sup>3</sup>H]RO6957022 binding was stable for at least 3 hours (Supplemental Figure 1) and reversible, as upon addition of 10  $\mu$ M of AM630 complete dissociation was achieved within 60 min (Fig. 3B). From the association and dissociation curves, the  $k_{on}$  value was determined to be  $0.11 \pm 0.01 \text{ nM}^{-1} \text{ min}^{-1}$ , while the  $k_{off}$  value was  $0.16 \pm 0.01 \text{ min}^{-1}$ , respectively. The latter resulted in a RT of  $6.3 \pm 0.5 \text{ min}$  (Table 1). Using the obtained  $k_{on}$  and  $k_{off}$  values, a kinetic  $K_D$  was determined to be 1.4 nM, which was in agreement with the equilibrium  $K_D$  and  $K_i$  values obtained from saturation and homologous displacement experiments, respectively.

*[<sup>3</sup>H]RO6957022 homologous competition association-* With the  $k_{on}$  ( $k_1$ ) and  $k_{off}$  ( $k_2$ ) values of [<sup>3</sup>H]RO6957022 already quantified, the  $k_{on}$  ( $k_3$ ) and  $k_{off}$  ( $k_4$ ) values for unlabeled RO6957022 were determined by performing homologous competition association experiments as a validation step (Fig. 5). For this purpose three different concentrations of RO6957022 were used to compete with [<sup>3</sup>H]RO6957022 (i.e. 1 nM, 3 nM and 9 nM), which corresponded to 0.3-, 1.0 and 3.0-fold  $IC_{50}$  concentrations, respectively. This resulted in  $k_{on}$  ( $k_3$ ) and  $k_{off}$  ( $k_4$ ) values for unlabeled RO6957022 of  $0.13 \pm 0.03 \text{ nM}^{-1} \text{ min}^{-1}$  and  $0.18 \pm 0.01 \text{ min}^{-1}$ , respectively (Table 2). Comparison of these values, as well as the calculated kinetic  $K_D$  and the other equilibrium and kinetic parameters obtained (Table 2), confirmed the accuracy of the [<sup>3</sup>H]RO6957022 competition association assay to determine the kinetics of unlabeled competitors at the CB<sub>2</sub>R. As a proof of concept, the obtained kinetic parameters derived from the shared analysis in presence of three concentrations of RO6957022, were compared with the  $k_3$  and  $k_4$  values determined with a single concentration (i.e. 1.0-fold  $IC_{50}$ ). Comparable values were achieved with only one concentration of competing unlabeled ligand (Table 2), therefore a similar approach was also applied for the following kinetic binding studies of other unlabeled competitors.

*Kinetic Binding profile determination of known synthetic CB<sub>2</sub> ligands-* Using the validated [<sup>3</sup>H]RO6957022 competition association assay, five of the eight CB<sub>2</sub>R ligands that were tested in a displacement assay (CP55,940, JWH-133, HU-308, GW405833 and SR144528) were selected to

MOL#108605

assess their kinetic binding profile (Fig. 6). [ $^3\text{H}$ ]RO6957022 association was challenged with 1.0-fold  $\text{IC}_{50}$  concentration of a competitor and typical competition association graphs were obtained (Fig.6). By fitting the kinetic binding parameters of [ $^3\text{H}$ ]RO6957022 in the model (Motulsky and Mahan, 1984), we were able to calculate association and dissociation rate constants for all tested CB2R ligands (Table 2). All full and partial agonists displayed dissociation kinetics at CB2R with high  $k_{\text{off}}$  values and thus a short RT; the latter was reflected by a typical shallow association curve in the presence of a quickly dissociating competitor. The association rate constants of the synthetic agonists, however, differed up to approximately 60-fold, to the extent that CP55,940 and GW405883 associated to CB2R faster and JWH-133 the slowest. Interestingly, the association curve obtained in the presence of SR144528, a CB2R inverse agonist, showed a characteristic ‘overshoot’ indicating a slower dissociation of SR144528 from the receptor relative to [ $^3\text{H}$ ]RO6957022 ( $k_{\text{off}} = 0.12 \pm 0.02 \text{ min}^{-1}$  vs.  $k_{\text{off}} = 0.19 \pm 0.03 \text{ min}^{-1}$ , respectively).

*Kinetic binding profile of endocannabinoids and noladin ether-* Lastly, we assessed the binding kinetics of the two major endocannabinoids on CB2R (Fig. 1), AEA and 2-AG, as well as a proposed endocannabinoid, noladin ether (NE). In competition association experiments with [ $^3\text{H}$ ]RO6957022, the three endocannabinoids displayed a distinct kinetic profile. As for the synthetic agonists, dissociation rate constants displayed moderate differences with AEA having the highest residence time of 1.4 min, followed by 2-AG and NE with 0.31 and 0.16 min, respectively (Fig. 7, Table 2). In contrast and similar to the synthetic agonists, endocannabinoid-receptor association rates were quite different, where 2-AG and NE had more than 10-fold higher  $k_{\text{on}}$  values than AEA.

*Correlation plots-* Considering that the affinity of a ligand is a function of its  $k_{\text{on}}$  and  $k_{\text{off}}$  value for a target, all the derived kinetic target affinities were compared with the corresponding equilibrium affinity values obtained with heterologous displacement experiments (Fig. 8A). A strong correlation ( $r = 0.984$ ,  $p < 0.0001$ ) between the negative logarithm of equilibrium affinity values ( $\text{pK}_i$ ) and kinetic affinity ( $\text{pK}_D$ ) values of all tested ligands was observed. Similarly, we plotted  $k_{\text{on}}$  (Fig. 8B) and  $k_{\text{off}}$  (Fig. 8C) values against the corresponding ligand affinities. From this a significant positive correlation was found between  $k_{\text{on}}$  and affinity values ( $r = 0.902$ ,  $p < 0.014$ ), on the other hand no correlation was

MOL#108605

found between affinity and  $k_{\text{off}}$  values ( $r = -0.177$ ,  $p < 0.738$ ). To visualize the relationship between a ligand's  $k_{\text{on}}$  and  $k_{\text{off}}$  values in regard to its affinity, a kinetic map was prepared (Fig. 8D), where compounds along the same diagonal lines show similar affinities, but have different kinetic properties. For instance, SR144528 and GW405833 displayed similar  $K_D$  values (i.e. located on same diagonal), but SR144528 has a slower dissociation rate, while GW405833 compensates its fast dissociation rate with an increased receptor association rate. Taken together, the kinetic map shows that each compound possesses a characteristic kinetic profile, which is not necessarily correlated to its affinity.

## Discussion

A decade after the (re)introduction of the concept of target residence time of drugs (Copeland et al., 2006), growing evidence has been accumulated on its potential implications in lead optimization when used prospectively (Guo et al., 2017). The concept behind receptor-ligand kinetics is to select candidate drugs based not only on their affinity, but also take their association and dissociation rates to and from their target into account (Copeland et al., 2006). However, when one desires to use a compounds' kinetic binding profile prospectively, kinetic binding assays are needed that often require radio- or fluorescently labeled tool compounds.

In this study we report the characterization of [ $^3\text{H}$ ]RO6957022, a novel high affinity radioligand with high selectivity for the human CB2R. Recently, an [ $^{11}\text{C}$ ] derivative of this compound has been reported as a PET imaging probe (Slavik et al., 2015). In that study, it was shown that reduced lipophilicity ( $\log D_{7.4} = 1.94$ ), high CB2R affinity ( $K_i = 2.5$  nM) and selectivity (<1000 times over hCB<sub>1</sub>) with a corresponding spleen-specific biodistribution made this compound a valuable tool for *in vivo* PET screenings. Another aspect that made [ $^3\text{H}$ ]RO6957022 a suitable tool compound for *in vitro* kinetic binding assays, is its inverse agonistic behavior. CB2R pharmacological studies are often performed in heterologous cell lines overexpressing the receptor. In these *in vitro* systems the increased receptor expression often is not accompanied by augmented G protein levels, therefore a large part of the receptor population is in its inactive form (Gonsiorek et al., 2006). This was true also

MOL#108605

for the employed cell line (i.e. CHO-K1\_hCB2), in which considerably high levels of CB2R were expressed as determined by saturation experiments (Table 1). In this scenario an inverse agonist radioligand is the preferred option for (kinetic) binding studies, as the biggest receptor subpopulation is targeted, which results in a larger assay window. This concept was also experimentally tested in parallel with the prototypical probe [<sup>3</sup>H]CP55,940 (Supplemental Figure 1). Although [<sup>3</sup>H]RO6957022 has a lower specific activity respect to [<sup>3</sup>H]CP55,940, both radioligands displayed comparable total binding signals, supporting the idea behind the use an inverse agonist for these studies. On the other hand, non-specific binding of [<sup>3</sup>H]RO6957022 was significantly lower, as expected from its aforementioned improved features, confirming the usefulness of this new probe for filtration binding studies.

Once the [<sup>3</sup>H]RO6957022 competition association assay was validated (Fig. 5), we selected representative compounds from the CB2R reference ligands, i.e. two full agonists (CP55,940 and JWH-133), a partial agonist (GW405833) and an inverse agonist (SR144528), for proof of concept. Using this [<sup>3</sup>H]RO6957022 assay we were able to determine the  $k_{on}$  and  $k_{off}$  values of all tested ligands. The derived kinetic  $K_D$  values obtained from these kinetic data were highly correlated to the obtained equilibrium  $K_i$  values (Fig. 8A), confirming the consistency of the kinetic binding data obtained with [<sup>3</sup>H]RO6957022. Among the tested ligands, SR144528 showed the longest residence time ( $RT = 8.7 \pm 1.7$  min) resulting in a characteristic, but small ‘overshoot’ of the competition association curve (Fig. 6). The present kinetic binding data together with the desirable pharmacokinetic features of SR144528, could explain its long lasting CB2R target occupancy reported in mouse spleen (Rinaldi-Carmona et al., 1998). Of note, as all measured receptor residence times are quite short (Table 2), the pharmacokinetics of these compounds is probably faster than their receptor residence time, which means that the latter parameter will probably not be (solely) driving their pharmacodynamics effects *in vivo* (Dahl and Akerud, 2013). However, the association rate constants exhibited a substantial spread, covering more than two log units among the studied CB2R synthetic and endogenous ligands, while the dissociation rates were more similar. Furthermore, as opposed to their dissociation rate constants, the association rate constants significantly correlate with  $K_i$  value,

MOL#108605

implying that the  $k_{on}$  value is the main driving force in CB2R affinity in the tested synthetic ligands. This is in contrast to a more common observation that target RT is the principal determinant for receptor affinity, as was reported on a number of targets, e.g.  $M_3$  (Sykes et al., 2009) and  $A_{2A}$  (Guo et al., 2012) receptors. There are some reports, however, where the influence of  $k_{on}$  value on affinity has been described. For instance, agonists for the  $\beta_2$ -adrenergic receptor (Sykes and Charlton, 2012) and modulators of the  $K_v11.1$  (hERG) channel (Yu et al., 2015a; Yu et al., 2015b) showed a similar correlation between  $k_{on}$  and affinity, where in the  $\beta_2$ -adrenergic receptor a role for the lipid membrane was postulated. This reinforces the notion that variations in  $k_{on}$  values can greatly impact the overall receptor affinity (de Witte et al., 2016; Vauquelin, 2016).

Considering the binding kinetic profile and physicochemical properties of the tested ligands, a phenomenon like rebinding and membrane interactions should also be taken into account, as it is likely to generate so called micro-pharmacokinetics and -dynamics in the proximity of CB2R, which can affect kinetic binding parameters. For AEA (Tian et al., 2005), and CP55,940 (Kimura et al., 2009), there is evidence that these ligands approach the CB2R by fast lateral diffusion from the membrane bilayer. This was substantiated in the recently published CB1R crystal structure, in which putative lipid access from the membrane bilayer was also described (Shao et al., 2016). Similarly, for AM841 (Pei et al., 2008), a CB2R covalent agonist, and 2-AG (Hurst et al., 2010) it has been shown that these ligands first distribute in the lipid bilayer and then bind and activate the receptor within microseconds (Hurst et al., 2010). The latter fits well with the high  $k_{on}$  value of 2-AG obtained in our kinetic binding experiments.

Lastly, in light of the high and dynamic endocannabinoid tone in healthy and especially in diseased states (Cabral and Griffin-Thomas, 2009), the characterization of the kinetic binding behavior of these endogenous ligands can reveal important insights about the physiology of these lipid mediators. Although the assessed affinities of the three endocannabinoids were in a close range ( $pK_D = 6.5 - 7.0$ ), significant differences were found in their kinetic binding profiles, i.e. 2-AG and NE showed a 10-fold higher  $k_{on}$  value for CB2R compared to AEA (Table 2, Fig. 7). Interestingly, their association rates appear to correlate to the described functional nature, i.e. 2-AG is a full agonist for the CB2R and



MOL#108605

AEA a partial agonist (Gonsiorek et al., 2000; Soethoudt et al., 2017). Moreover, the obtained molecular evidence of the endocannabinoid-CB2R binding kinetics fits with the on-demand nature of the ECS (Di Marzo, 2009), where endocannabinoids are rapidly and locally synthesized or degraded, which allows for swift receptor binding without a prolonged functional effect (Piomelli, 2003). Considering the substantial paracrine concentrations of 2-AG, together with its high  $k_{on}$  value towards CB2R, it can be speculated that this endocannabinoid will quickly achieve effective target occupancy (Schoop and Dey, 2015). Furthermore, CB2R has been reported to rapidly undergo to desensitization (Bouaboula et al., 1999). With this in mind, a more transient receptor activation would be favorable for an effective but safe physiological action.

Therefore, the question arises whether a long or short RT would be most desirable for the CB2R. The short RTs of the endogenous cannabinoids (Table 2) may constitute a clue already, as knowing the binding kinetics of a target's endogenous ligands could give important information for a proper pharmacological intervention (Nederpelt et al., 2016). Likewise the high  $k_{on}$  values and short RTs found for the synthetic ligands in Table 2 are reminiscent of what has already been described for other molecular targets (Copeland, 2010), in which a pulse (i.e. fast  $k_{on}$  and  $k_{off}$ ) rather than sustained target occupancy by an antagonist is beneficial to achieve desirable pharmacological outcomes and reduced side effects. An example of the latter is the dopamine D<sub>2</sub> receptor (Pan et al., 2008). For this target a positive correlation was found between extrapyramidal side effects and prolonged receptor blockade by long RT antagonists (Seeman, 2005), possibly due to the continued suppression of the sub-cortical dopaminergic activity (Casey, 2004). Analogously, pharmacological interventions on CB2R should consider the local mediator function of endocannabinoids (Di Marzo, 2008) in physiology and their pivotal role in immunomodulation. Specifically, CB2R activation triggers a complex signal cascade that can either reduce the early phases of the immune response (Herring et al., 1998) through inhibition of adenylyl cyclase or induce immunosuppression through apoptosis mechanisms (Eisenstein et al., 2007). To date, the inhibitory effects of cannabinoids on the immune system are known to be transient (Pandey et al., 2009), allowing the immune response to be quickly restored for potential infectious threats. Therefore, although speculative, long RT CB2R agonists as well as

MOL#108605

antagonists would not be desirable, as they would continuously interfere with ECS homeostasis, ultimately leading to adverse effects.

## Conclusions

We have characterized a novel high affinity inverse agonist radioligand for human CB2R, the 2,5,6-substituted pyridine derivative [<sup>3</sup>H]RO695702. Its CB2R binding properties have been validated in equilibrium saturation and displacement assays, as well as kinetically in (competition) association and dissociation assays. Using a variety of CB2R reference ligands, we showed that [<sup>3</sup>H]RO6957022 is an excellent tool compound to determine ligand affinities and kinetic rate constants at CB2R, including for the first time the kinetic binding profiles of the CB2R endogenous ligands. The latter gives important insights on the mechanism of action of these mediators of such paramount lipid signaling. This improved knowledge of ECS physiology can be translated into a better therapeutic drug design strategy. Thus, with the introduction of [<sup>3</sup>H]RO6957022 we hope to aid and stimulate the development and kinetic optimization of ligands for CB2R in early drug discovery.

MOL#108605

## Acknowledgments

The authors would like to thank Mathias Müller for his contribution in the synthesis of [<sup>3</sup>H]RO6957022.

## Author contributions

Participated in research design: A.C.R., U.G., J.F., C.U., A.M., M.S., L.H.H., A.P.I.

Conducted experiments: A.M, H.S.

Contributed new reagents or analytic tools: U.G., T.H., M.S.

Performed data analysis: A.M., H.S., A.C.R.

Wrote or contributed to the writing of the manuscript: A.M., A.C.R., U.G., J.F., C.U., M.S., L.H.H., A.P.I.

MOL#108605

## References

- Anand P, Whiteside G, Fowler CJ and Hohmann AG (2009) Targeting CB2 receptors and the endocannabinoid system for the treatment of pain. *Brain Res Rev* **60**(1): 255-266.
- Aso E, Juves S, Maldonado R and Ferrer I (2013) CB2 cannabinoid receptor agonist ameliorates Alzheimer-like phenotype in AbetaPP/PS1 mice. *J Alzheimers Dis* **35**(4): 847-858.
- Benesty J, Chen J, Huang Y and Cohen I (2009) Pearson Correlation Coefficient, in *Noise Reduction in Speech Processing* pp 1-4, Springer Berlin Heidelberg, Berlin, Heidelberg.
- Bouaboula M, Dussosoy D and Casellas P (1999) Regulation of Peripheral Cannabinoid Receptor CB2 Phosphorylation by the Inverse Agonist SR 144528: Implications for receptor biological responses. *Journal of Biological Chemistry* **274**(29): 20397-20405.
- Brown SM, Wager-Miller J and Mackie K (2002) Cloning and molecular characterization of the rat CB2 cannabinoid receptor. *Biochimica et Biophysica Acta (BBA) - Gene Structure and Expression* **1576**(3): 255-264.
- Cabral GA and Griffin-Thomas L (2009) Emerging Role of the CB(2) Cannabinoid Receptor in Immune Regulation and Therapeutic Prospects. *Expert reviews in molecular medicine* **11**: e3-e3.
- Cabral GA, Raborn ES, Griffin L, Dennis J and Marciano-Cabral F (2008) CB2 receptors in the brain: role in central immune function. *Br J Pharmacol* **153**(2): 240-251.
- Casey DE (2004) Pathophysiology of Antipsychotic Drug-Induced Movement Disorders. *The Journal of clinical psychiatry* **65**(suppl 9): 25-28.
- Cheng YC and Prusoff WH (1973) Relationship between the inhibition constant (K<sub>i</sub>) and the concentration of inhibitor which causes 50 per cent inhibition (I<sub>50</sub>) of an enzymatic reaction. *Biochemical pharmacology* **22**(23): 3099-3108.
- Copeland RA (2010) The dynamics of drug-target interactions: drug-target residence time and its impact on efficacy and safety. *Expert Opinion on Drug Discovery* **5**(4): 305-310.
- Copeland RA, Pompliano DL and Meek TD (2006) Drug-target residence time and its implications for lead optimization. *Nat Rev Drug Discov* **5**(9): 730-739.
- Dahl G and Akerud T (2013) Pharmacokinetics and the drug-target residence time concept. *Drug Discovery Today* **18**(15-16): 697-707.
- de Witte WEA, Danhof M, van der Graaf PH and de Lange ECM (2016) In vivo Target Residence Time and Kinetic Selectivity: The Association Rate Constant as Determinant. *Trends in Pharmacological Sciences* **37**(10): 831-842.
- Devane WA, Dysarz FA, III, Johnson MR, Melvin LS and Howlett AC (1988) Determination and characterization of a cannabinoid receptor in rat brain. *Mol Pharmacol* **34**(5): 605-613.
- Dhopeswarkar A and Mackie K (2014) CB2 Cannabinoid Receptors as a Therapeutic Target—What Does the Future Hold? *Molecular Pharmacology* **86**(4): 430-437.
- Di Marzo V (2008) Targeting the endocannabinoid system: to enhance or reduce? *Nat Rev Drug Discov* **7**(5): 438-455.
- Di Marzo V (2009) The endocannabinoid system: Its general strategy of action, tools for its pharmacological manipulation and potential therapeutic exploitation. *Pharmacological Research* **60**(2): 77-84.
- Di Marzo V and Fontana A (1995) Anandamide, an endogenous cannabinomimetic eicosanoid: 'killing two birds with one stone'. *Prostaglandins, Leukotrienes and Essential Fatty Acids* **53**(1): 1-11.
- Eisenstein TK, Meissler JJ, Wilson Q, Gaughan JP and Adler MW (2007) Anandamide and Δ(9)-Tetrahydrocannabinol Directly Inhibit Cells of the Immune System via CB(2) Receptors. *Journal of neuroimmunology* **189**(1-2): 17-22.
- Fernandez-Ruiz J, Moreno-Martet M, Rodriguez-Cueto C, Palomo-Garo C, Gomez-Canas M, Valdeolivas S, Guaza C, Romero J, Guzman M, Mechoulam R and Ramos JA (2011) Prospects for cannabinoid therapies in basal ganglia disorders. *Br J Pharmacol* **163**(7): 1365-1378.
- Galiegue S, Mary S, Marchand J, Dussosoy D, Carriere D, Carayon P, Bouaboula M, Shire D, Le Fur G and Casellas P (1995) Expression of central and peripheral cannabinoid receptors in human immune tissues and leukocyte subpopulations. *Eur J Biochem* **232**(1): 54-61.

MOL#108605

- Gaoni Y and Mechoulam R (1964) Isolation, Structure, and Partial Synthesis of an Active Constituent of Hashish. *Journal of the American Chemical Society* **86**(8): 1646-1647.
- Gonsiorek W, Hesk D, Chen S-C, Kinsley D, Fine JS, Jackson JV, Bober LA, Deno G, Bian H, Fossetta J, Lunn CA, Kozlowski JA, Lavey B, Piwinski J, Narula SK, Lundell DJ and Hipkin RW (2006) Characterization of Peripheral Human Cannabinoid Receptor (hCB2) Expression and Pharmacology Using a Novel Radioligand, [35S]Sch225336. *Journal of Biological Chemistry* **281**(38): 28143-28151.
- Gonsiorek W, Lunn C, Fan XD, Narula S, Lundell D and Hipkin RW (2000) Endocannabinoid 2-arachidonyl glycerol is a full agonist through human type 2 cannabinoid receptor: Antagonism by anandamide. *Molecular Pharmacology* **57**(5): 1045-1050.
- Guindon J and Hohmann AG (2008) Cannabinoid CB2 receptors: a therapeutic target for the treatment of inflammatory and neuropathic pain. *Br J Pharmacol* **153**(2): 319-334.
- Guo D, Heitman LH and Ijzerman AP (2017) Kinetic Aspects of the Interaction between Ligand and G Protein-Coupled Receptor: The Case of the Adenosine Receptors. *Chemical Reviews* **117**(1): 38-66.
- Guo D, Mulder-Krieger T, Ijzerman AP and Heitman LH (2012) Functional efficacy of adenosine A(2A) receptor agonists is positively correlated to their receptor residence time. *British Journal of Pharmacology* **166**(6): 1846-1859.
- Herring AC, Koh WS and Kaminski NE (1998) Inhibition of the Cyclic AMP Signaling Cascade and Nuclear Factor Binding to CRE and  $\kappa$ B Elements by Cannabinol, a Minimally CNS-Active Cannabinoid. *Biochemical Pharmacology* **55**(7): 1013-1023.
- Horvath B, Magid L, Mukhopadhyay P, Batkai S, Rajesh M, Park O, Tanchian G, Gao RY, Goodfellow CE, Glass M, Mechoulam R and Pacher P (2012) A new cannabinoid CB2 receptor agonist HU-910 attenuates oxidative stress, inflammation and cell death associated with hepatic ischaemia/reperfusion injury. *Br J Pharmacol* **165**(8): 2462-2478.
- Hurst DP, Grossfield A, Lynch DL, Feller S, Romo TD, Gawrisch K, Pitman MC and Reggio PH (2010) A lipid pathway for ligand binding is necessary for a cannabinoid G protein-coupled receptor. *Journal of Biological Chemistry*.
- Kimura T, Cheng K, Rice KC and Gawrisch K (2009) Location, Structure, and Dynamics of the Synthetic Cannabinoid Ligand CP-55,940 in Lipid Bilayers. *Biophysical Journal* **96**(12): 4916-4924.
- Li Q, Wang F, Zhang Y-M, Zhou J-J and Zhang Y (2013) Activation of Cannabinoid Type 2 Receptor by JWH133 Protects Heart Against Ischemia/Reperfusion-Induced Apoptosis. *Cellular Physiology and Biochemistry* **31**(4-5): 693-702.
- Ligresti A, De Petrocellis L and Di Marzo V (2016) From Phytocannabinoids to Cannabinoid Receptors and Endocannabinoids: Pleiotropic Physiological and Pathological Roles Through Complex Pharmacology. *Physiological Reviews* **96**(4): 1593-1659.
- Lotersztajn S, Teixeira-Clerc F, Julien B, Deveaux V, Ichigotani Y, Manin S, Tran-Van-Nhieu J, Karsak M, Zimmer A and Mallat A (2008) CB2 receptors as new therapeutic targets for liver diseases. *Br J Pharmacol* **153**(2): 286-289.
- Ludden TM, Beal SL and Sheiner LB (1994) Comparison of the Akaike Information Criterion, the Schwarz criterion and the F test as guides to model selection. *Journal of Pharmacokinetics and Biopharmaceutics* **22**(5): 431-445.
- Mechoulam R, Hanus LO, Pertwee R and Howlett AC (2014) Early phytocannabinoid chemistry to endocannabinoids and beyond. *Nat Rev Neurosci* **15**(11): 757-764.
- Morales P, Hernandez-Folgado L, Goya P and Jagerovic N (2016) Cannabinoid receptor 2 (CB2) agonists and antagonists: a patent update. *Expert Opin Ther Pat* **26**(7): 843-856.
- Moris D, Georgopoulos S, Felekouras E, Patsouris E and Theocharis S (2015) The effect of endocannabinoid system in ischemia-reperfusion injury: a friend or a foe? *Expert Opinion on Therapeutic Targets* **19**(9): 1261-1275.
- Motulsky HJ and Mahan LC (1984) The kinetics of competitive radioligand binding predicted by the law of mass action. *Molecular Pharmacology* **25**(1): 1-9.

MOL#108605

- Mukhopadhyay P, Baggelaar M, Erdelyi K, Cao Z, Cinar R, Fezza F, Ignatowska-Janlowska B, Wilkerson J, van Gils N, Hansen T, Ruben M, Soethoudt M, Heitman L, Kunos G, Maccarrone M, Lichtman A, Pacher P and Van der Stelt M (2016) The novel, orally available and peripherally restricted selective cannabinoid CB2 receptor agonist LEI-101 prevents cisplatin-induced nephrotoxicity. *British Journal of Pharmacology* **173**(3): 446-458.
- Mukhopadhyay P, Rajesh M, Pan H, Patel V, Mukhopadhyay B, Batkai S, Gao B, Hasko G and Pacher P (2010) Cannabinoid-2 receptor limits inflammation, oxidative/nitrosative stress, and cell death in nephropathy. *Free Radic Biol Med* **48**(3): 457-467.
- Munro S, Thomas KL and Abu-Shaar M (1993) Molecular characterization of a peripheral receptor for cannabinoids. *Nature* **365**(6441): 61-65.
- Nederpelt I, Bleeker D, Tuijt B, Ijzerman AP and Heitman LH (2016) Kinetic binding and activation profiles of endogenous tachykinins targeting the NK1 receptor. *Biochemical Pharmacology* **118**: 88-95.
- Ofek O, Karsak M, Leclerc N, Fogel M, Frenkel B, Wright K, Tam J, Attar-Namdar M, Kram V, Shohami E, Mechoulam R, Zimmer A and Bab I (2006) Peripheral cannabinoid receptor, CB2, regulates bone mass. *Proc Natl Acad Sci U S A* **103**(3): 696-701.
- Pan B, Hillard CJ and Liu Q-s (2008) D2 Dopamine Receptor Activation Facilitates Endocannabinoid-Mediated Long-Term Synaptic Depression of GABAergic Synaptic Transmission in Midbrain Dopamine Neurons via cAMP-Protein Kinase A Signaling. *The Journal of Neuroscience* **28**(52): 14018-14030.
- Pandey R, Mousawy K, Nagarkatti M and Nagarkatti P (2009) Endocannabinoids and immune regulation. *Pharmacological Research* **60**(2): 85-92.
- Pei Y, Mercier RW, Anday JK, Thakur GA, Zvonok AM, Hurst D, Reggio PH, Janero DR and Makriyannis A (2008) Ligand-Binding Architecture of Human CB2 Cannabinoid Receptor: Evidence for Receptor Subtype-Specific Binding Motif and Modeling GPCR Activation. *Chemistry & biology* **15**(11): 1207-1219.
- Picone RP and Kendall DA (2015) Minireview: From the Bench, Toward the Clinic: Therapeutic Opportunities for Cannabinoid Receptor Modulation. *Molecular Endocrinology* **29**(6): 801-813.
- Piomelli D (2003) The molecular logic of endocannabinoid signalling. *Nat Rev Neurosci* **4**(11): 873-884.
- Riether D (2012) Selective cannabinoid receptor 2 modulators: a patent review 2009--present. *Expert Opin Ther Pat* **22**(5): 495-510.
- Rinaldi-Carmona M, Barth F, Millan J, Derocq J-M, Casellas P, Congy C, Oustric D, Sarran M, Bouaboula M, Calandra B, Portier M, Shire D, Brelière J-C and Fur GL (1998) SR 144528, the First Potent and Selective Antagonist of the CB2 Cannabinoid Receptor. *Journal of Pharmacology and Experimental Therapeutics* **284**(2): 644-650.
- Schoop A and Dey F (2015) On-rate based optimization of structure-kinetic relationship – surfing the kinetic map. *Drug Discovery Today: Technologies* **17**: 9-15.
- Seeman P (2005) An Update of Fast-Off Dopamine D2 Atypical Antipsychotics. *American Journal of Psychiatry* **162**(10): 1984-a-1985.
- Shao Z, Yin J, Chapman K, Grzemska M, Clark L, Wang J and Rosenbaum DM (2016) High-resolution crystal structure of the human CB1 cannabinoid receptor. *Nature* **540**(7634): 602-606.
- Slavik R, Grether U, Müller Herde A, Gobbi L, Fingerle J, Ullmer C, Krämer SD, Schibli R, Mu L and Ametamey SM (2015) Discovery of a High Affinity and Selective Pyridine Analog as a Potential Positron Emission Tomography Imaging Agent for Cannabinoid Type 2 Receptor. *Journal of Medicinal Chemistry* **58**(10): 4266-4277.
- Smith PK, Krohn RI, Hermanson GT, Mallia AK, Gartner FH, Provenzano MD, Fujimoto EK, Goeke NM, Olson BJ and Klenk DC (1985) Measurement of protein using bicinchoninic acid. *Analytical Biochemistry* **150**(1): 76-85.
- Soethoudt M, Grether U, Fingerle J, Grim TW, Fezza F, de Petrocellis L, Ullmer C, Rothenhäusler B, Perret C, van Gils N, Finlay D, MacDonald C, Chicca A, Gens MD, Stuart J, de Vries H,

MOL#108605

- Mastrangelo N, Xia L, Alachouzos G, Baggelaar MP, Martella A, Mock ED, Deng H, Heitman LH, Connor M, Di Marzo V, Gertsch J, Lichtman AH, Maccarrone M, Pacher P, Glass M and van der Stelt M (2017) Cannabinoid CB2 receptor ligand profiling reveals biased signalling and off-target activity. *Nature Communications* **8**: 13958.
- Sykes DA and Charlton SJ (2012) Slow receptor dissociation is not a key factor in the duration of action of inhaled long-acting  $\beta(2)$ -adrenoceptor agonists. *British Journal of Pharmacology* **165**(8): 2672-2683.
- Sykes DA, Dowling MR and Charlton SJ (2009) Exploring the Mechanism of Agonist Efficacy: A Relationship between Efficacy and Agonist Dissociation Rate at the Muscarinic M<sub>3</sub> Receptor. *Molecular Pharmacology* **76**(3): 543-551.
- Sykes DA, Parry C, Reilly J, Wright P, Fairhurst RA and Charlton SJ (2014) Observed Drug-Receptor Association Rates Are Governed by Membrane Affinity: The Importance of Establishing “Micro-Pharmacokinetic/Pharmacodynamic Relationships” at the  $\beta 2$ -Adrenoceptor. *Molecular Pharmacology* **85**(4): 608-617.
- Tian X, Guo J, Yao F, Yang D-P and Makriyannis A (2005) The Conformation, Location, and Dynamic Properties of the Endocannabinoid Ligand Anandamide in a Membrane Bilayer. *Journal of Biological Chemistry* **280**(33): 29788-29795.
- Tummino PJ and Copeland RA (2008) Residence time of receptor-ligand complexes and its effect on biological function. *Biochemistry* **47**(20): 5481-5492.
- Turcotte C, Blanchet M-R, Laviolette M and Flamand N (2016) The CB2 receptor and its role as a regulator of inflammation. *Cellular and Molecular Life Sciences* **73**(23): 4449-4470.
- Vauquelin G (2016) Effects of target binding kinetics on in vivo drug efficacy: koff, kon and rebinding. *British Journal of Pharmacology* **173**(15): 2319-2334.
- Yu Z, Ijzerman AP and Heitman LH (2015a) K(v)11.1 (hERG)-induced cardiotoxicity: a molecular insight from a binding kinetics study of prototypical K(v)11.1 (hERG) inhibitors. *British Journal of Pharmacology* **172**(3): 940-955.
- Yu Z, van Veldhoven JPD, Louvel J, 't Hart IME, Rook MB, van der Heyden MAG, Heitman LH and Ijzerman AP (2015b) Structure–Affinity Relationships (SARs) and Structure–Kinetics Relationships (SKRs) of Kv11.1 Blockers. *Journal of Medicinal Chemistry* **58**(15): 5916-5929.

## Footnotes

U.G., C.U., T.H. and A.C.R. are employees of F. Hoffmann-La Roche Ltd.



## Legends for Figures

**Fig. 1.** *Chemical structures of the tested CB<sub>2</sub>R ligands.* The present compound selection included synthetic full (i.e. RO6957022, CP55,940, HU-308, AM1241), partial (i.e. GW405833) and inverse agonists (i.e. SR144528, AM630), as well as endogenous CB<sub>2</sub>R ligands (i.e. 2-AG, AEA and noladin ether).

**Fig. 2.** *Binding assay optimization and window determination of [<sup>3</sup>H]RO6957022 to CHO-K1 hCB<sub>2</sub> membranes.* Initially, various assay buffers and filter pre-treatments were tested (A) to reduce non-specific and filter binding. Once the optimal assay condition was determined (i.e. 50 mM Tris-HCl pH 7.4 and 0.1% BSA and filters prewetted with PEI), receptor specificity was tested comparing total binding (TB) and non-specific binding (NSB) using 15 µg membranes from CHOK1\_hCB2 and mock control (B). Data are representative of the ratio between TB and NSB (dashed line), statistical comparisons were carried out with an unpaired student *t*-test for each experimental group (\*\* *p* < 0.01). Single point binding experiments were performed to determine the optimal membrane concentration in terms of specific window and ligand depletion limit (dashed line) (C). Data are shown as mean and the standard error of the mean (S.E.M) from three independent experiments performed in duplicate.

**Fig. 3.** *Equilibrium and kinetic characterization of [<sup>3</sup>H]RO6957022 binding.* (A) Representative saturation binding experiment of [<sup>3</sup>H]RO6957022 in either absence (closed circles) or presence (open circles) of 10 µM AM630 to determine non-specific binding. (B) Association and dissociation experiment with 3 nM [<sup>3</sup>H]RO6957022 interacting with CHO-K1\_hCB<sub>2</sub> membranes at 25°C. Dissociation of the radioligand was initiated by addition of 10 µM AM630 (final concentration) after equilibrium had been reached. Association and dissociation rate constants were best fitted using a one-phase association or dissociation model, where data are represented as the mean and the S.E.M. of six independent experiments performed in duplicate.

**Fig. 4.** *Binding affinity determination of reference CB<sub>2</sub> ligands using [<sup>3</sup>H]RO6957022.* Heterologous displacement experiments on CHO-K1\_hCB<sub>2</sub> membranes using a selection of CB<sub>2</sub> full (CP55,940,

JWH-133, AM1241, HU-308), partial (GW405833) and inverse agonists (SR144528, AM630), including homologous displacement of [ $^3\text{H}$ ]RO6957022. Data are shown as the mean and the S.E.M. of three independent displacement experiments each performed in duplicate.

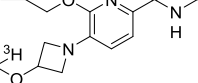
**Fig. 5.** *Homologous competition association of [ $^3\text{H}$ ]RO6957022.* Competition association experiment of [ $^3\text{H}$ ]RO6957022 on CHO-K1\_hCB<sub>2</sub> membranes using three concentrations (0.3-, 1.0- and 3.0-fold IC<sub>50</sub>) of its unlabeled congener. Data are shown as the average and the S.E.M. of seven independent experiments each performed in duplicate.

**Fig. 6.** *Kinetic binding experiments of well-known CB<sub>2</sub> ligands.* Competition association of [ $^3\text{H}$ ]RO6957022 on CHO-K1\_hCB<sub>2</sub> membranes at 25°C in either absence (control) or presence of a single concentration (i.e. IC<sub>50</sub> value) of CP55,940, JWH-133, HU-308, GW405833 or SR144528. Data are shown as the mean and the S.E.M. of three independent experiments each performed in duplicate.

**Fig. 7.** *Kinetic binding behavior of the endogenous ligands at hCB<sub>2</sub> receptor.* Competition association of [ $^3\text{H}$ ]RO6957022 on CHO-K1\_hCB<sub>2</sub> membranes at 25°C in either absence (control) or presence of a single concentration (i.e. IC<sub>50</sub> value) of anandamide (AEA), 2-arachidonoylglycerol (2-AG) or noladin ether (NE). Data are shown as mean and the S.E.M. of six independent experiments each performed in duplicate.

**Fig. 8.** *Correlation plots of equilibrium and kinetic parameters of reference CB<sub>2</sub> ligands.* (A) Negative logarithmic transformation of affinities determined by equilibrium displacement (pK<sub>i</sub>) versus kinetic binding (pK<sub>D</sub>); (B) Correlation between logarithmic association rate (log k<sub>on</sub>, M<sup>-1</sup> min<sup>-1</sup>) and pK<sub>i</sub> (C) Correlation between logarithmic dissociation rate (log k<sub>off</sub>, min<sup>-1</sup>) and pK<sub>i</sub>; (D) Kinetic map in which k<sub>on</sub> values are plotted against k<sub>off</sub> values. Grey diagonal lines indicate an identical affinity (K<sub>D</sub>) value for different k<sub>off</sub>/k<sub>on</sub> combinations. Data are shown as the average values from **Table 2** without error bars to provide clarity.

## Tables

		$k_{on}$ ( $nM^{-1} min^{-1}$ )	$k_{off}$ ( $min^{-1}$ )	$RT$ ( $min$ )	$K_D, K_i$ ( $nM$ )	$B_{max}$ ( $pmol/mg$ protein)
Binding assay	Association <sup>a</sup>	$0.11 \pm 0.01$	-	-	-	-
	Dissociation <sup>b</sup>	-	$0.16 \pm 0.01$	$6.3 \pm 0.5$	$1.4 \pm 0.2$	-
	Competition association (three concentrations) <sup>c</sup>	$0.13 \pm 0.03$	$0.18 \pm 0.01$	$5.5 \pm 0.3$	$1.4 \pm 0.3$	-
	Competition association (one concentration) <sup>d</sup>	$0.15 \pm 0.03$	$0.19 \pm 0.03$	$5.3 \pm 0.7$	$1.3 \pm 0.4$	-
	Saturation <sup>e</sup>	-	-	-	$1.7 \pm 0.1$	$25 \pm 1$
	Displacement <sup>f</sup>	-	-	-	$1.3 \pm 0.1$	-

Data shown are presented as the mean  $\pm$  S.E.M. of at least three individual experiments.

<sup>a</sup> Association rate constants as determined with [<sup>3</sup>H]RO6957022 (for corresponding graph see **Fig. 3B**)

<sup>b</sup> Dissociation rate constants as determined with [<sup>3</sup>H]RO6957022 (for corresponding graph see **Fig. 3B**).

<sup>c</sup> Competition association with three concentrations (0.3-, 1.0-, 3.0-fold IC<sub>50</sub>) of cold RO6957022 (for corresponding graph see **Fig. 4**).  $K_D = k_{off}/k_{on}$

<sup>d</sup> Competition association with a single concentration (1.0-fold IC<sub>50</sub>) of cold RO6957022 (for corresponding graph see **Fig. 4**).  $K_D = k_{off}/k_{on}$

<sup>e</sup> K<sub>D</sub> value obtained from saturation binding of [<sup>3</sup>H]RO6957022 (for corresponding graph see **Fig. 3A**)

<sup>f</sup> K<sub>i</sub> value obtained from homologous displacement of cold RO6957022 by [<sup>3</sup>H]RO6957022 (for corresponding graph see **Fig. 4**).

**Table 2.** Affinity and kinetic binding proprieties of CB2R reference ligands determined by [<sup>3</sup>H]RO6957022 displacement and competition association experiments.

Compound	$pK_i$ ( $K_i$ in nM)	$k_{on}$ ( $nM^{-1} min^{-1}$ )	$k_{off}$ ( $min^{-1}$ )	$RT$ (min)	$K_D$ (nM)
RO6957022	$8.9 \pm 0.05$ (1.2)	$0.15 \pm 0.03$	$0.19 \pm 0.03$	$5.3 \pm 0.7$	$1.3 \pm 0.4$
CP55,940	$9.3 \pm 0.03$ (0.50)	$0.22 \pm 0.02$	$0.20 \pm 0.02$	$5.0 \pm 0.4$	$0.90 \pm 0.1$
JWH-133	$7.4 \pm 0.07$ (39)	$0.0042 \pm 0.001$	$0.31 \pm 0.07$	$3.2 \pm 0.7$	$75 \pm 24$
HU-308	$7.6 \pm 0.08$ (25)	$0.011 \pm 0.001$	$0.23 \pm 0.01$	$4.2 \pm 0.2$	$21 \pm 3$
AM1241	$8.2 \pm 0.03$ (6.3)	-	-	-	-
GW405833	$8.4 \pm 0.02$ (3.5)	$0.25 \pm 0.06$	$0.70 \pm 0.1$	$1.4 \pm 0.3$	$2.8 \pm 0.8$
SR144528	$8.3 \pm 0.02$ (5.0)	$0.028 \pm 0.003$	$0.12 \pm 0.02$	$8.7 \pm 1.7$	$4.1 \pm 0.9$
AM630	$7.7 \pm 0.03$ (20)	-	-	-	-
Anandamide (AEA)	-	$0.0024 \pm 0.0004$	$0.73 \pm 0.11$	$1.4 \pm 0.2$	$305 \pm 45$
2-Arachidonoylglycerol (2-AG)	-	$0.032 \pm 0.005$	$3.2 \pm 0.9$	$0.31 \pm 0.09$	$99 \pm 27$
Noladin ether (NE)	-	$0.042 \pm 0.033$	$6.3 \pm 1.0$	$0.16 \pm 0.03$	$151 \pm 24$

Receptor affinities ( $K_i$ ) were calculated using the Cheng- Prusoff equation (Cheng and Prusoff, 1973). Kinetic binding parameters (i.e.  $k_{on}$ ,  $k_{off}$ ) were obtained using Motulsky-Mahan model (Motulsky and Mahan, 1984), the derived affinity values were calculated using the equation  $K_D = k_{off}/k_{on}$ . The results shown are the mean  $\pm$  S.E.M. of at least three individual experiments.

## Figures

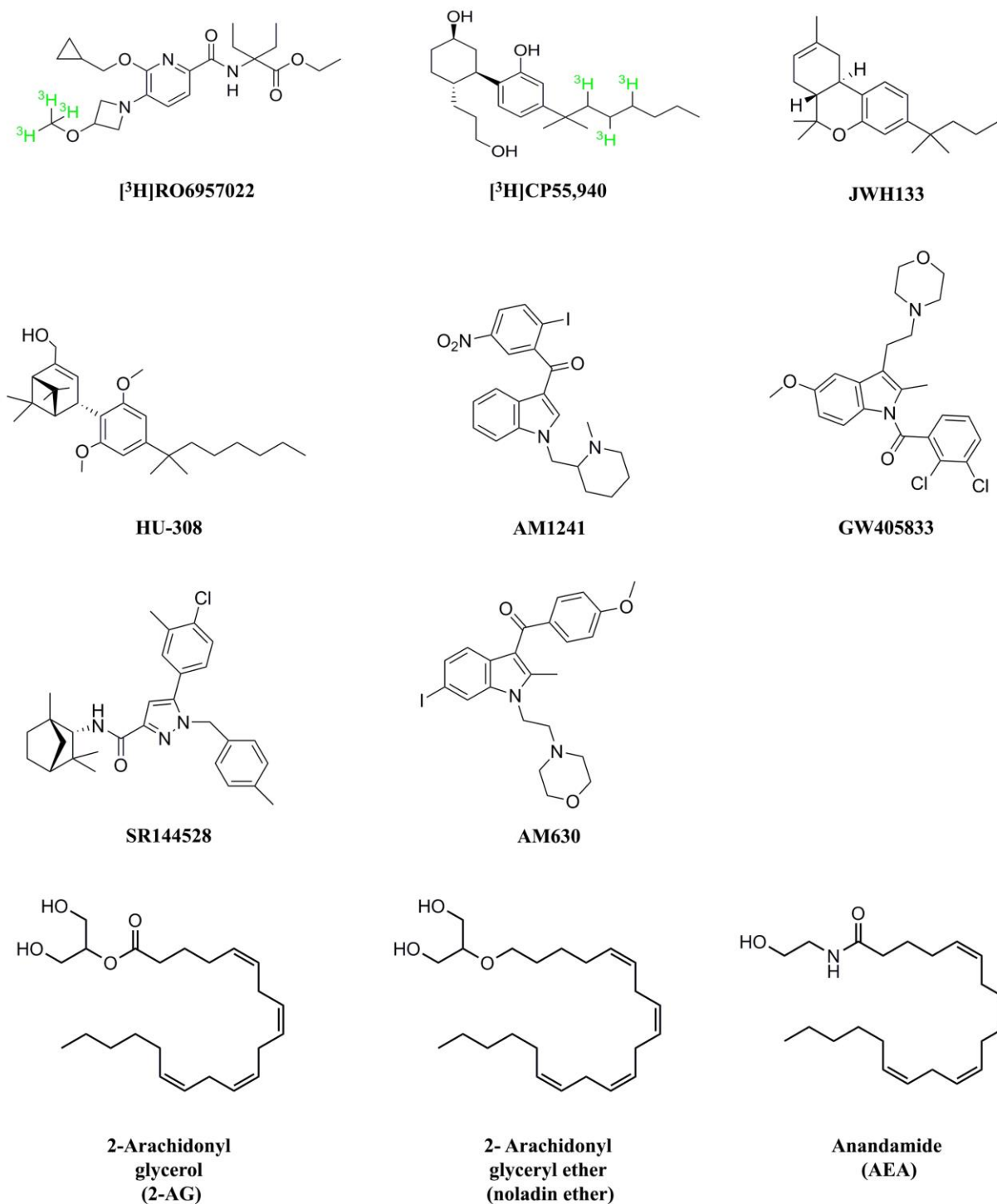
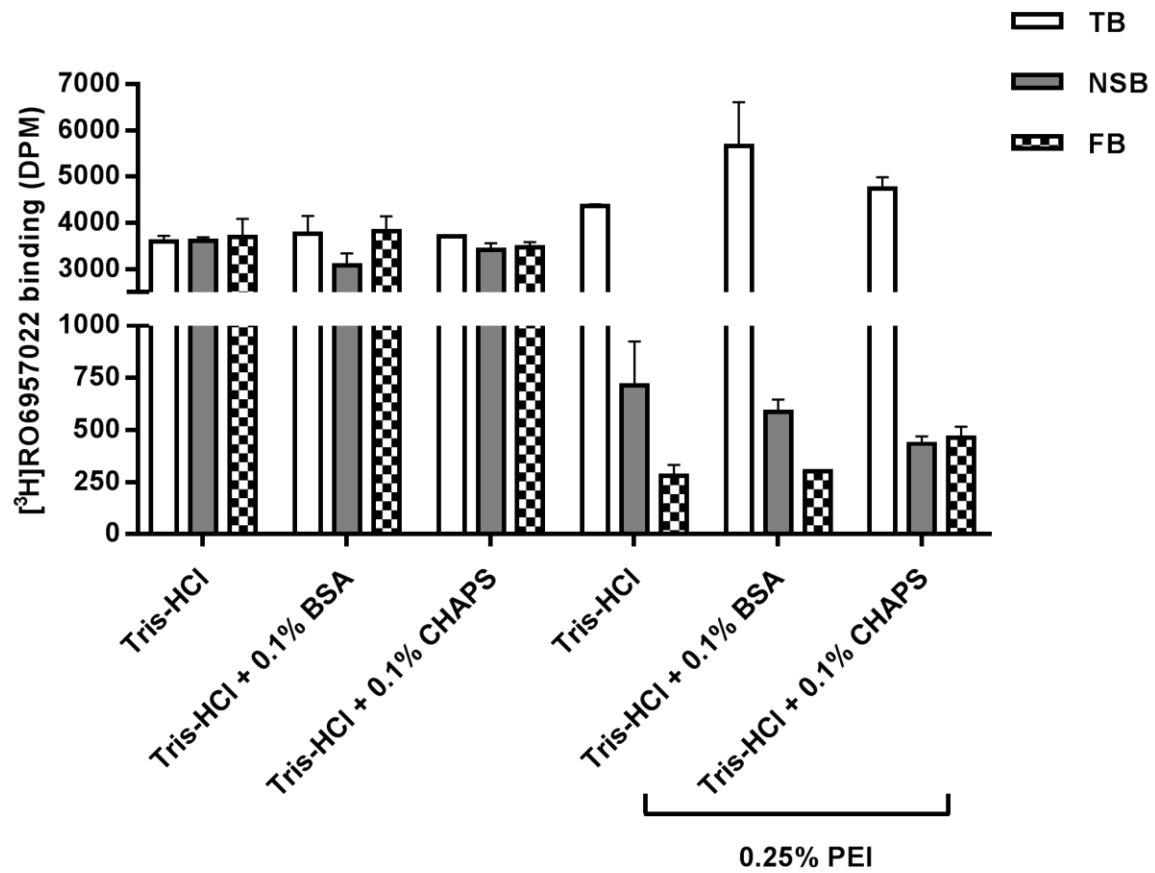
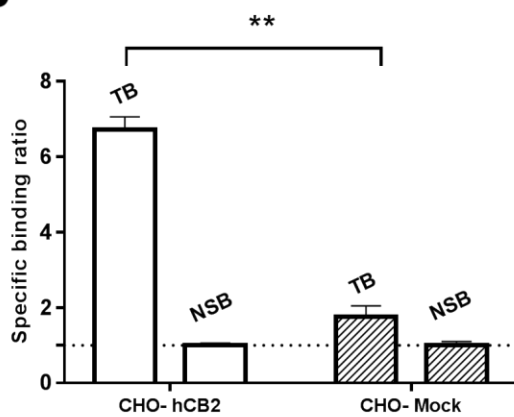


**Figure 1**

**A**



**B**



**C**

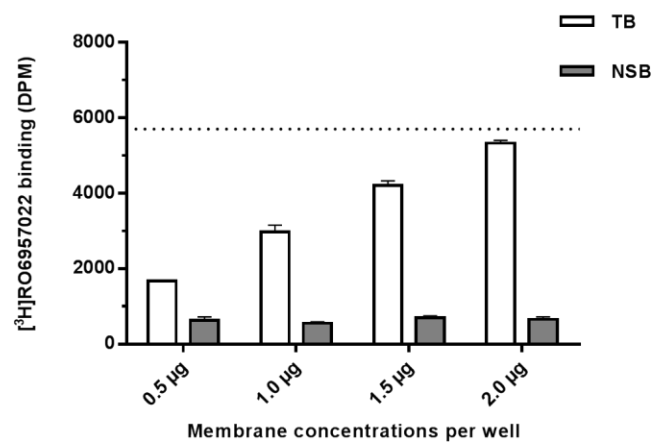
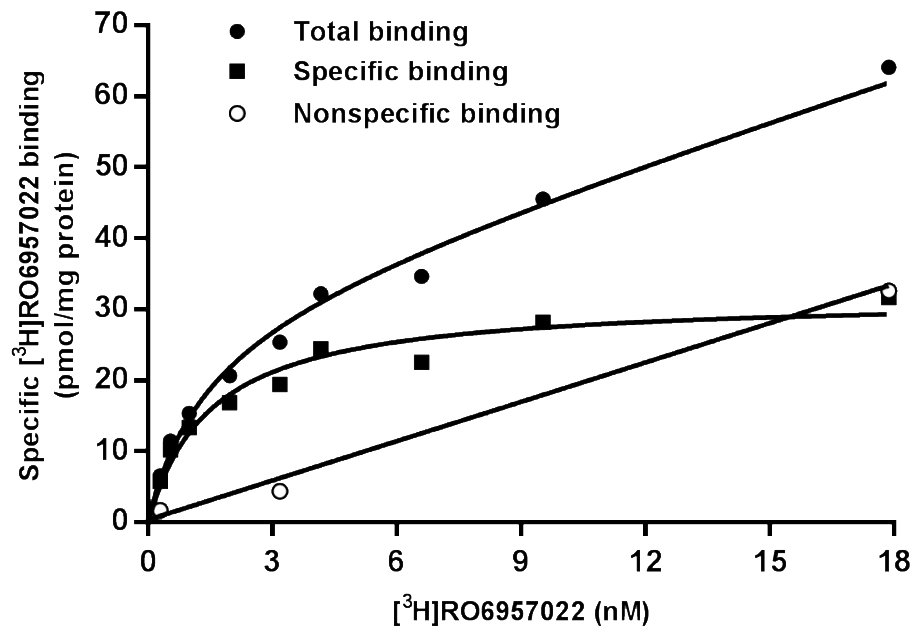


**Figure 2**

**A**



**B**

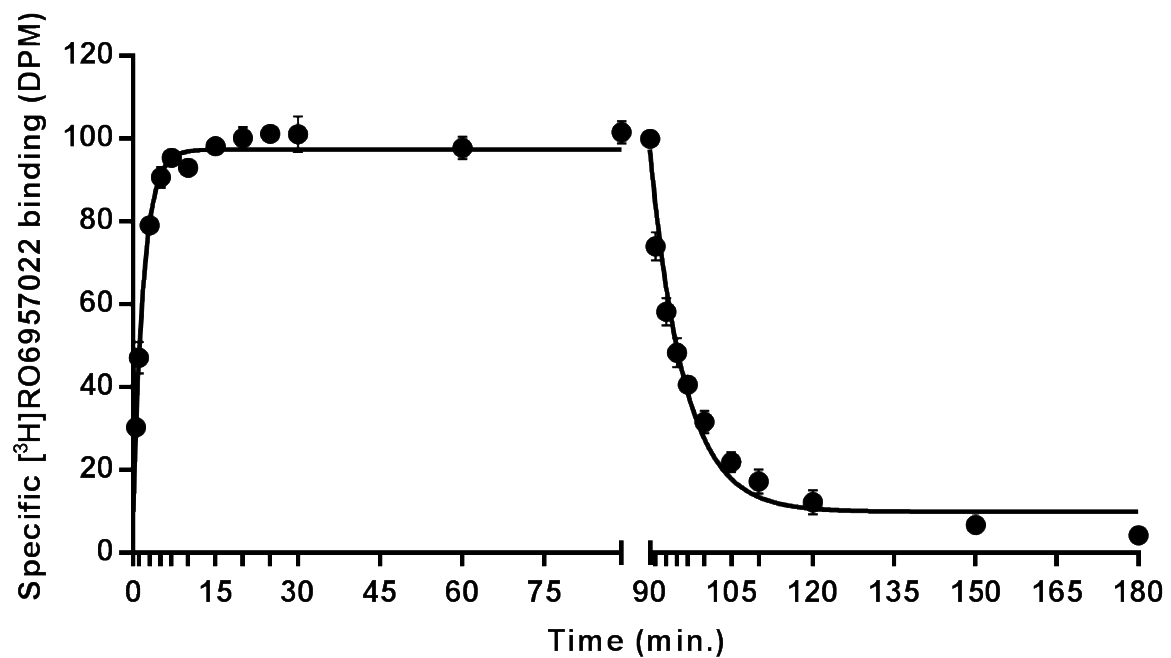


**Figure 3**

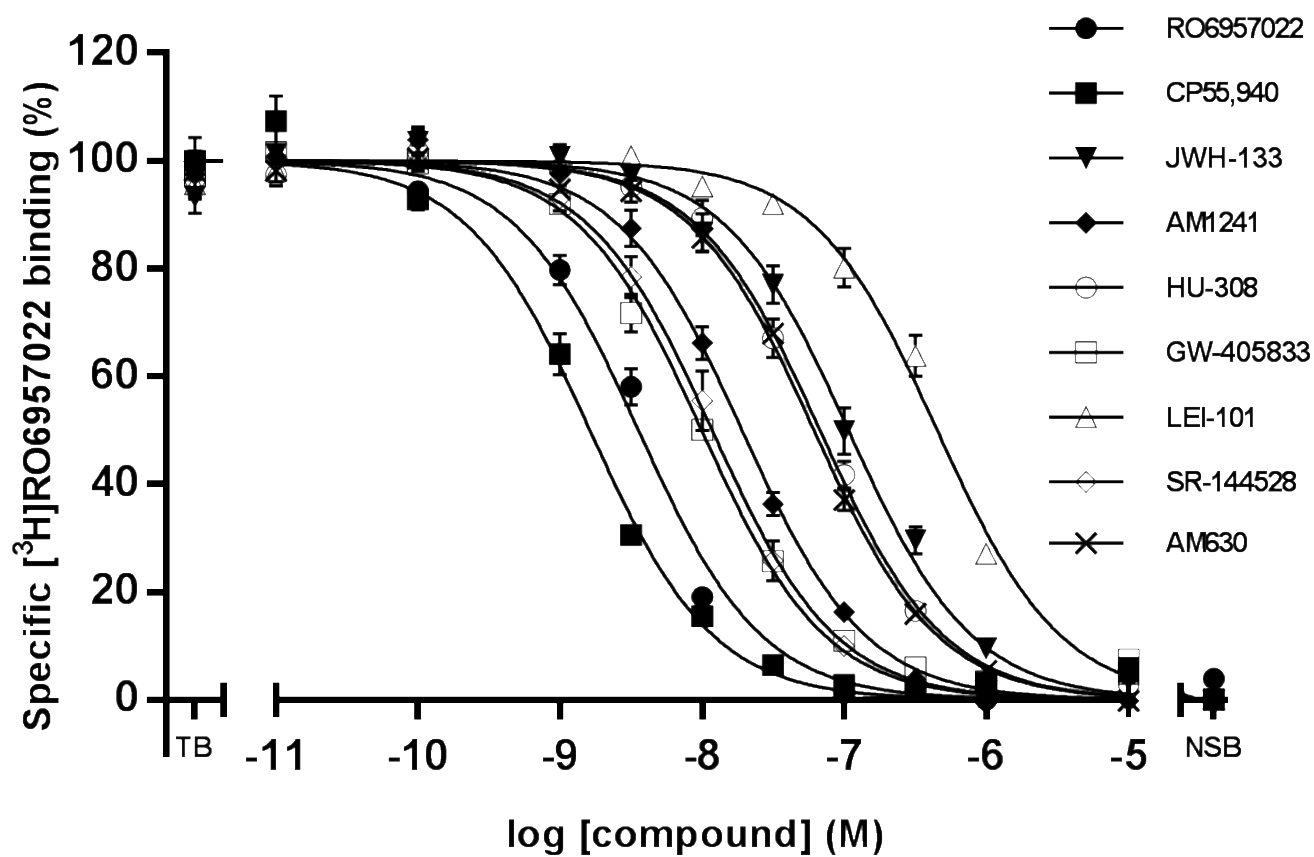


**Figure 4**



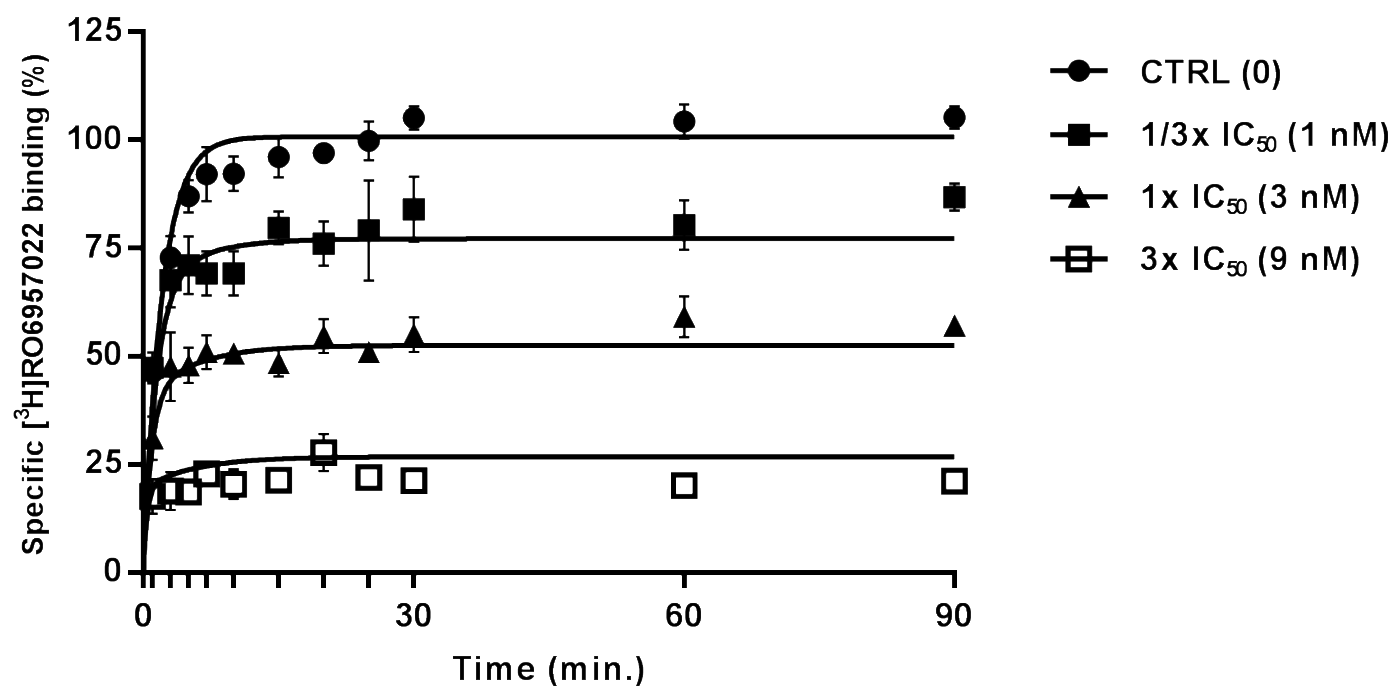


**Figure 5**

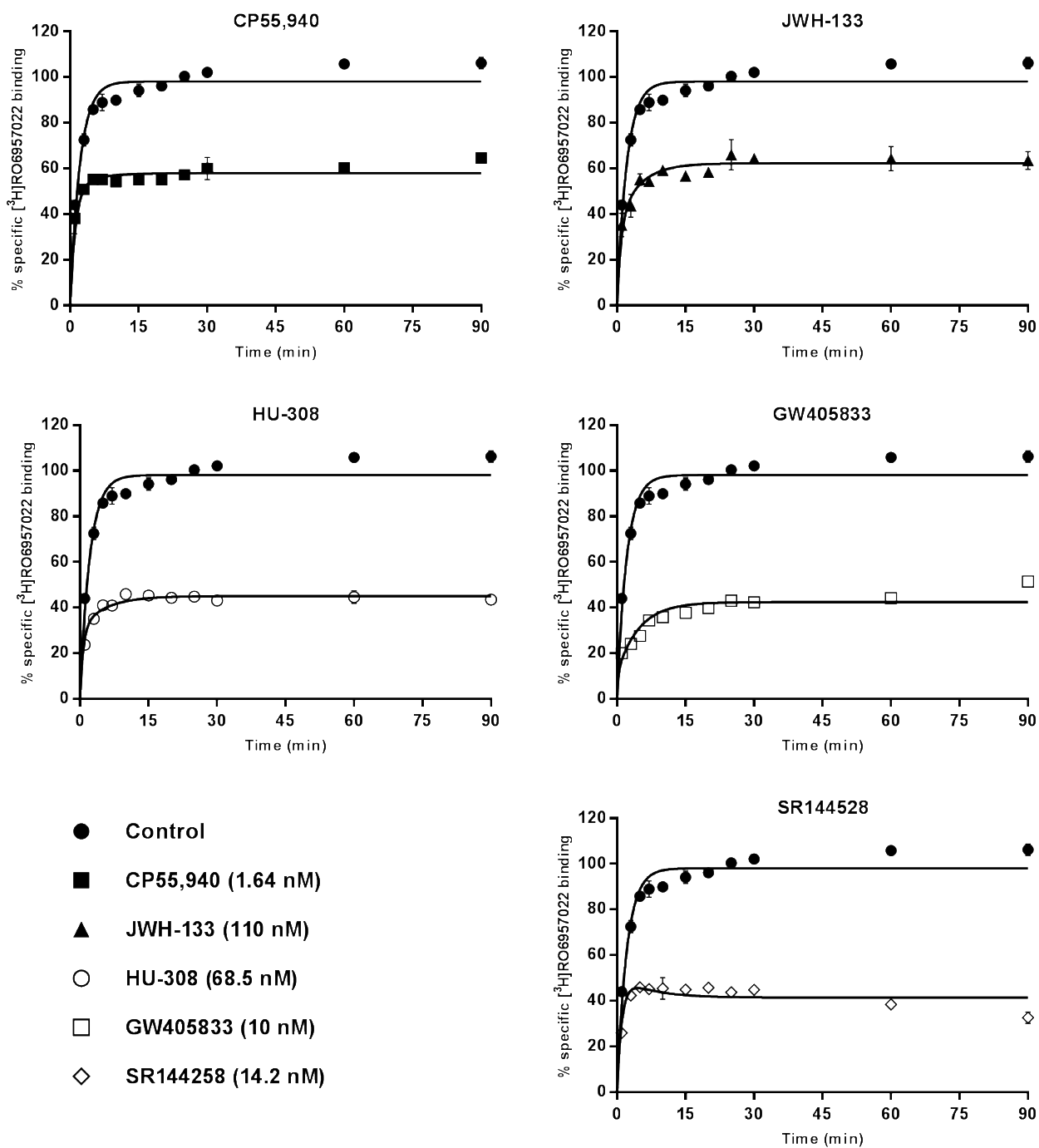


**Figure 6**

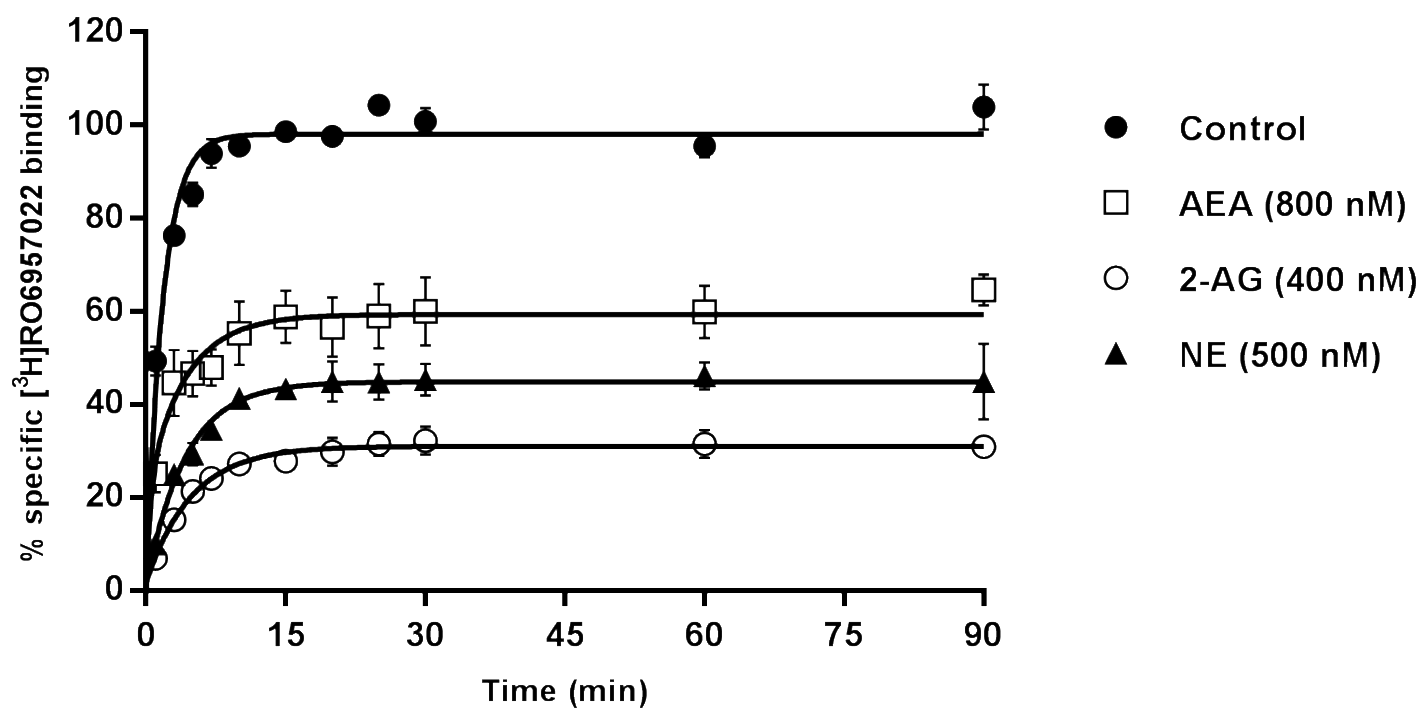


**Figure 7**

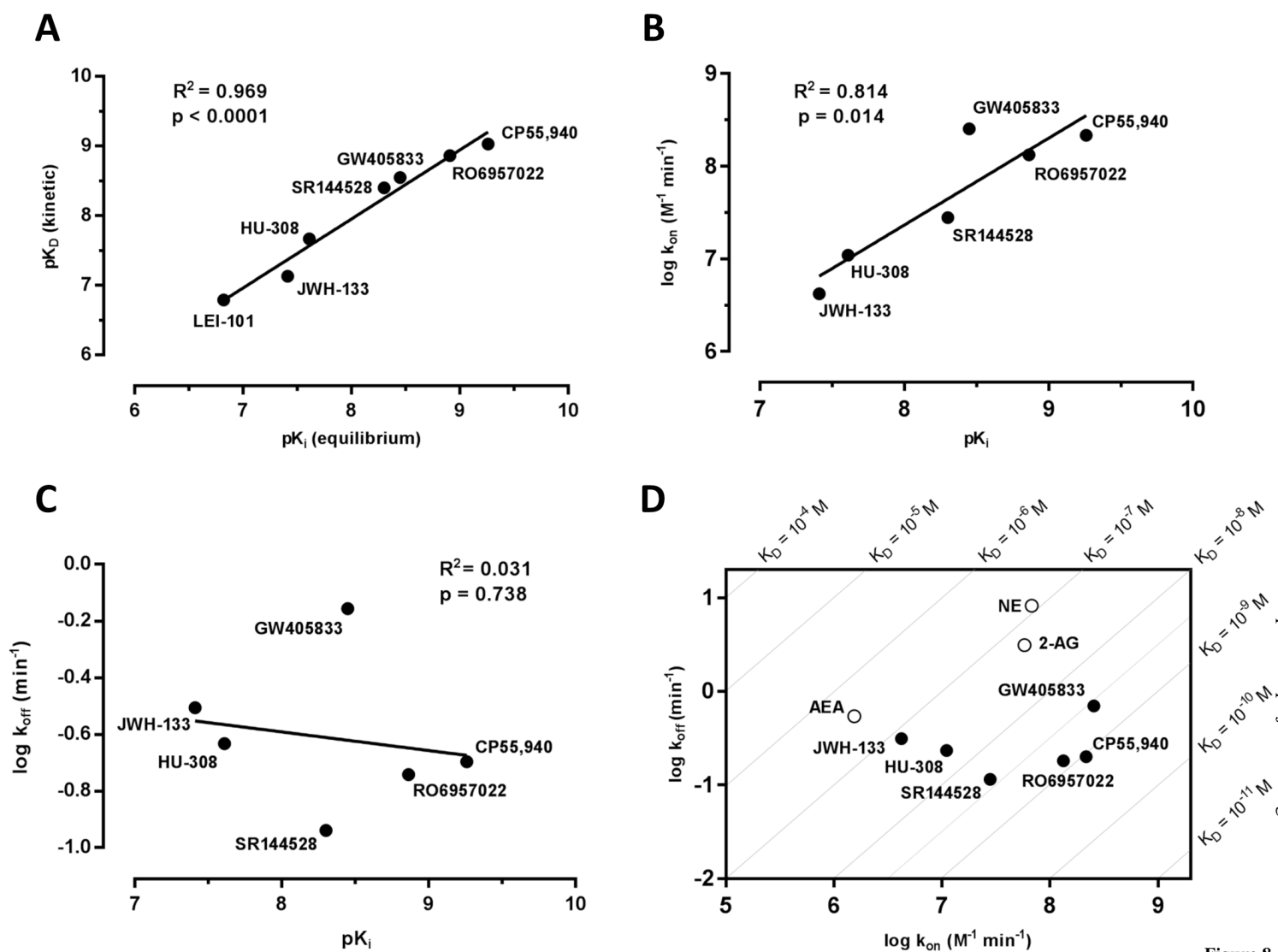
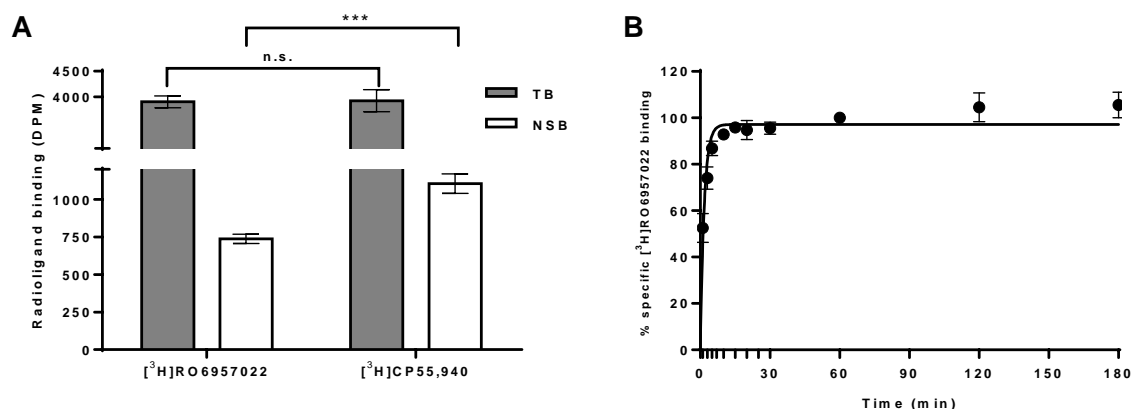


Figure 8

## A novel selective inverse agonist of the CB2 receptor as a radiolabeled tool compound for kinetic binding studies.

Andrea Martella, Huub Sijben, Arne C. Rufer, Uwe Grether, Juergen Fingerle, Christoph Ullmer, Thomas Hartung, Adriaan P. IJzerman, Mario van der Stelt and Laura H. Heitman



**Sup. Fig.1.** Filtration binding comparison between  $[^3\text{H}]\text{RO6957022}$  and  $[^3\text{H}]\text{CP55,940}$ . Total (TB) and non-specific (NSB) binding, were determined in the absence or presence of AM630 (10  $\mu\text{M}$ ), respectively (A). Similar assay conditions (i.e. Tris-HCl 50 mM, pH 7.4 (25°C) and 0.1% BSA) were used for both radioligands, except for  $\text{MgCl}_2$  (5 mM) added to the  $[^3\text{H}]\text{CP55,940}$  samples. Data are shown as mean  $\pm$  S.E.M. of three independent experiments performed in duplicate; statistical significance was determined by student *t*-test (\*\*\*  $p \leq 0.001$ ). Please note the differences in specific activity for both radioligands ( $[^3\text{H}]\text{RO6957022}$ , 83.7 Ci/mmol, and  $[^3\text{H}]\text{CP55,940}$ , 150.2 Ci/mmol). Prolonged binding association experiment with 3 nM  $[^3\text{H}]\text{RO6957022}$  interacting with CHO-K1\_hCB<sub>2</sub> membranes at 25°C (B). Data are shown as mean  $\pm$  S.E.M. of three independent experiments.